Light vectors coupled to bosonic currents

Jeff A. Dror,[1,2,*] Robert Lasenby,[3,†] and Maxim Pospelov[4,5,‡]

[1]*Department of Physics, University of California, Berkeley, California 94720, USA*
[2]*Ernest Orlando Lawrence Berkeley National Laboratory,*
University of California, Berkeley, California 94720, USA
[3]*Stanford Institute for Theoretical Physics, Stanford University, Stanford, California 94305, USA*
[4]*Perimeter Institute for Theoretical Physics, 31 Caroline Street N, Waterloo, Ontario N2L 2Y5, Canada*
[5]*Department of Physics and Astronomy, University of Victoria,*
Victoria, British Columbia V8P 5C2, Canada

New spin-1 particles with masses below the weak scale are present in many theories of beyond Standard Model (SM) physics. In this work, we extend previous analyses by systematically considering the couplings of such a vector to the bosonic sector of the SM, focusing on models that lead to mass mixing with the Z boson. These couplings generically lead to enhanced emission of the vector's longitudinal mode, both in Higgs decays and in flavor changing meson decays. We present bounds in the SM + X effective theory and investigate their model dependence. For the case of Higgs decays, we point out that tree-level vector emission is, depending on the model, not always enhanced, affecting the constraints. For meson decays, which are the dominant constraints at small vector masses, we find that while B decay constraints can be weakened by fine-tuning UV parameters, it is generically difficult to suppress the stringent constraints from kaon decays.

I. INTRODUCTION

Light new states, with masses below the weak scale, arise in many theories of physics beyond the Standard Model (SM). These may have gone undetected if their couplings to the SM are sufficiently weak. If such particles are not associated with many other new states at the same mass scale, then they should generically have spin ≤ 1; here, we will concentrate on new light vector bosons, which have been extensively studied as mediators to a dark sector [1–3], and as explanations for experimental anomalies [4–9].

The lowest-dimensional interaction between a new vector and SM states is the dimension-4 coupling to a SM current, $X_\mu J_{\rm SM}^\mu$. Unless $J_{\rm SM}$ is conserved, including quantum effects, the SM + X effective theory is non-renormalizable. This manifests as (energy/m_X)-enhanced amplitudes involving the longitudinal mode of X, for processes with $\partial_\mu J^\mu \neq 0$. Such processes can be the

dominant X production mechanism at high-energy colliders, mostly importantly through emission in flavor changing neutral current (FCNC) B and K decays.

In previous works [10,11], we systematically considered the phenomenological consequences of general couplings to SM fermions, $X_\mu J_{{\rm SM},f}^\mu$. The only fully conserved currents in the SM are the electromagnetic (EM) current, and (if neutrinos are Dirac) the $B - L$ current; any other coupling will give rise to enhanced longitudinal emission in some circumstances (though if nonconservation is only through neutrino masses, e.g., for $L_\mu - L_\tau$, this will be very suppressed). Various models have been considered in the literature; light vectors having a chiral anomaly with the SM [10–12] (see also [13,14] for vectors above the weak scale), vectors with axial couplings [5,11,15–18], and ones with weak-isospin violation [11,18].

Here, we extend our previous analyses by considering light vectors with couplings to bosonic SM fields. In particular, an XW^+W^- coupling will contribute to emission in FCNC penguin amplitudes, leading to similar phenomenology as for couplings to fermions[1] [11]. New phenomenology can also arise from a coupling to the SM Higgs, leading to exotic Higgs decays. Such effects have been

---

[*]jdror@lbl.gov
[†]rlasenby@stanford.edu
[‡]mpospelov@perimeterinstitute.ca

---

[1]We can write the W^+W^- current as a sum of the EM current and a fermionic current, showing that longitudinal emission is the same as for the fermionic current.

considered in a number of previous papers [19–21]; in this work, we consider the possibilities more systematically, investigating how signatures vary across different models.

For calculational simplicity, we will mostly work with UV completions that do not introduce extra electroweak symmetry breaking (EWSB). This means that, in the SM + X effective field theory (EFT), X must couple to a SM-gauge-invariant current (or via Wess-Zumino terms, which are determined by the SM fermion couplings of X [10,11]). The lowest-dimension couplings with nontrivial effects are

$$J_{\text{SM,b}}^{\mu} = \partial_{\nu} B^{\mu\nu}; \quad \partial^{\mu}(H^{\dagger}H); \quad H^{\dagger} i \overset{\leftrightarrow}{D}{}^{\mu} H; \quad H^{\dagger} i \overset{\leftrightarrow}{D}{}_{X}^{\mu} H, \quad (1)$$

where D^{μ} corresponds to the SM covariant derivative and D_{X}^{μ} includes a $U(1)_X$ contribution, $D_{X}^{\mu} \equiv D^{\mu} + i g_X X^{\mu}/2$. The first current in (1) is the familiar "kinetic mixing" operator [22], and upon the use of equations of motion for B_{μ} can be replaced with the hypercharge current J_{Y}^{μ}. The $X_{\mu} \partial^{\mu}(H^{\dagger}H)$ coupling is equivalent, on integration by parts, to $-(\partial^{\mu} X_{\mu}) H^{\dagger} H$, and replacing $\partial^{\mu} X_{\mu}$ via the equations of motion gives a higher-dimensional operator.

The $H^{\dagger} D_{(X)} H$ currents are of more interest [the subscript (X) is used to denote either the SM or SM + $U(1)_X$]. In the unitary gauge, they lead to a mass mixing of X with the Z boson,

$$\mathcal{L} \supset g_X X_{\mu} (H^{\dagger} i \overset{\leftrightarrow}{D}{}_{(X)}^{\mu} H) \rightarrow \varepsilon_Z m_Z^2 X_{\mu} Z^{\mu}. \quad (2)$$

Transforming to the mass basis, this results in the light vector state gaining a coupling to the SM neutral current. In particular, this gives a coupling to W^+W^-, resulting in FCNC decays, and a coupling to the Higgs, resulting in exotic Higgs decays. Consequently, the mass mixing coupling provides an excellent prototype for the phenomenology of enhanced longitudinal emission. This coupling has also been the subject of several phenomenological studies (see, e.g., [19–21,23–33]), including motivations for new parity-violation experiments [21,34,35].

Previous studies of $X - Z$ mixing have generally assumed that it leads to $1/m_X$-enhanced amplitudes for $h \rightarrow ZX$ at tree level [19–21]. This is true if $\varepsilon_Z m_Z^2 X_{\mu} Z^{\mu}$ is the only operator in the EFT, but not if it arises from the SM-gauge-invariant operators above. If we were to ignore the SM Yukawa couplings, then $H^{\dagger} D_{(X)} H$ would be conserved within the SM.[2] Consequently, the tree-level $h \rightarrow XZ$ amplitude is *suppressed* at small m_X. To obtain significant $1/m_X$-enhanced amplitudes, we need to consider processes involving heavy fermions. Examples

---

[2]This is true for both currents for single X emission, though $H^{\dagger}DH$ is not conserved in processes involving multiple X's, with consequences, e.g., in $h \rightarrow XX$.

include FCNC penguin amplitudes, and Higgs decays through a top loop, which we will study in detail.

The $h \rightarrow ZX$ amplitude is finite at one loop, so the rate for this processes is predicted in the EFT, up to corrections suppressed by the scale of heavier states. However, FCNC penguin amplitudes (and $h \rightarrow XX$) are divergent at one loop. Hence, in the limit that the scale of new states Λ is significantly higher than the EW scale, the dominant contribution to the amplitude will scale as $\log(\Lambda^2/m_{\text{EW}}^2)$. For SM-gauge-invariant X couplings, the coefficient of this term is determined within the EFT. There will also be threshold corrections from the high-scale physics, which are not suppressed by inverse powers of Λ. Both of these effects mean that, without knowledge of the UV physics, only a generic prediction can be made for FCNC amplitudes.

If Λ is not too high, then the log-enhanced term may be numerically comparable to other contributions. In particular, one might worry that there could be cancellations between this piece and other contributions, significantly altering the rates for meson decays. In this work, we illustrate the robustness of FCNC constraints within a two Higgs doublet model (2HDM), though we expect our conclusions to hold more generally. While $B \rightarrow KX$ rates can be suppressed by tuning the 2HDM parameters (in particular, the mass of the charged Higgs), $K^{\pm} \rightarrow \pi^{\pm} X$ amplitudes can only be suppressed by a factor of a few, unless the model has additional flavor structure.

The $1/m_X$-enhanced amplitudes under discussion arise from the nonrenormalizability of the SM + X EFT, which must have a cutoff at (or below) a scale parametrically set by m_X/g_X. Standard UV completions, such as the 2HDM examples given later, result in higher-dimensional EFT operators involving X being suppressed by g_X, as well as by inverse powers of the cutoff scale. Hence, the effects of dimension > 4 operators are less important.

II. FURTHER COMMENTS ON BOSONIC CURRENT PORTAL

The $H^{\dagger} D_{(X)} H$ couplings have the following unitary gauge decomposition:

$$g_X X_{\mu} H^{\dagger} i \overset{\leftrightarrow}{D}{}^{\mu} H = m_Z^2 \left(1 + \frac{h}{v}\right)^2 \varepsilon_Z X_{\mu} Z^{\mu}, \quad (3)$$

$$g_X X_{\mu} H^{\dagger} i \overset{\leftrightarrow}{D}{}_{X}^{\mu} H = m_Z^2 \left(1 + \frac{h}{v}\right)^2 (\varepsilon_Z Z_{\mu} + \varepsilon_Z^2 X_{\mu}) X^{\mu}, \quad (4)$$

where $v \simeq 246$ GeV is the electroweak vacuum expectation value (VEV), h is the physical (125 GeV) Higgs boson, and $\varepsilon_Z \equiv g_X v/m_Z$. The additional contribution in D_X leads to terms proportional to $X_{\mu} X^{\mu}$, resulting in the current being conserved even in processes involving multiple X's (but still no SM Yukawa insertions). As mentioned above, this

form is somewhat deceiving as one may expect it to lead to unsuppressed $hX_\mu X^\mu$ and $hX_\mu Z^\mu$ couplings. To see this is not the case we work in the mass basis where we parametrize the couplings as

$$\mathcal{L} \supset C_{hXZ}\left(\frac{h}{v} + \frac{1}{2}\frac{h^2}{v^2}\right)X_\mu Z^\mu$$
$$+ \frac{1}{2}C_{hXX}\left(\frac{h}{v} + \frac{1}{2}\frac{h^2}{v^2}\right)X_\mu X^\mu, \qquad (5)$$

where the relation between the Higgs and Higgs-squared couplings is guaranteed by assuming that the direction of electroweak symmetry breaking is aligned with the Higgs. We find

$$
\begin{array}{lll}
C_{hXZ} = -2\varepsilon_Z m_X^2, & C_{hXX} = 2\varepsilon_Z^2 m_X^4/m_Z^2 & (H^\dagger D_X H) \\
C_{hXZ} = -2\varepsilon_Z m_X^2, & C_{hXX} = 2\varepsilon_Z^2 m_Z^2 & (H^\dagger D H).
\end{array} \qquad (6)
$$

We conclude that the $\mathcal{M}_{h\to ZX} \propto m_X^{-1}$ is not a generic consequence of ZX mass mixing, as it cancels for the simplest SM-gauge-invariant realization. Notice, however, that if such mixing is realized as part of a more complicated current, e.g., $X_\mu(H^\dagger i\overset{\leftrightarrow}{D}{}^\mu H)(H^\dagger H) \supset Z_\mu X^\mu$, m_X^{-1} behavior can appear even at tree level. This is because $(H^\dagger i\overset{\leftrightarrow}{D}{}^\mu H)(H^\dagger H)$ is not conserved in the purely bosonic sector. Similarly, if there are additional sources of EWSB, then this spoils the conservation of the $U(1)_X$ current and can also lead to enhanced rates (as discussed below in the case of a 2HDM model).

While important for Higgs physics, these couplings with h will not affect the one-loop results for the FCNC amplitudes. Therefore, the mass mixing $X_\mu Z^\mu$ operator and full SM-gauge-invariant couplings, $X \cdot H^\dagger D_{(X)} H$, at leading loop level will give identical answers for FCNCs (as will any model having the same XW^+W^- and X-quark vertices). Nevertheless, the SM-gauge-invariant theory is more convenient for calculations, as it allows these to be performed in arbitrary gauges. Keeping the Goldstone modes in the Lagrangian, in addition to the couplings in (3) or (4), we have

$$\mathcal{L} \supset \frac{1}{2}g_X X^\mu(G^+ i\partial_\mu G^- - gvG^+ W_\mu^- + \ldots) + \text{H.c.} \quad (7)$$

where the ellipses denote neutral component terms which will not be relevant for us here.

It is instructive to discuss possible UV completions of (3) and (4). If the breaking of $U(1)_X$ occurs at a high energy scale Λ, then the vector portal under discussion is itself an effective operator,

$$\frac{1}{\Lambda^2}(\Phi^* i\overset{\leftrightarrow}{D}{}^\mu \Phi)(H^\dagger i\overset{\leftrightarrow}{D}{}^\mu H) \to g_X X_\mu(H^\dagger i\overset{\leftrightarrow}{D}{}^\mu H), \quad (8)$$

where Φ is the "dark" Higgs of $U(1)_X$, and D_μ between Φ^* and Φ is the covariant derivative with respect to $U(1)_X$, $D^\mu = \partial^\mu + ig'X^\mu$, so that the coupling X used previously relates to the $U(1)_X$ charge g' as $g_X = g'|\langle\Phi\rangle|^2/\Lambda^2$. Such couplings of X were discussed in e.g., [36]. While explicitly and separately SM and $U(1)_X$ invariant, operator (8) is of dimension 6 and needs further UV completion. A straightforward UV completion can be built using sets of heavy vectorlike fermions: N_{SM} (charged only under SM), N_X [charged only under $U(1)_X$], and N (singlet under all gauge symmetries). The charges are assigned in such a way that $\Phi N N_X$ and HNN_{SM} Yukawa interactions are allowed. This way, one fermionic loop of the $N - N_X - N_{SM}$ mixed propagator creates (8), and the effective energy scale that would resolve this interaction is linked to the fermion masses.

A UV completion of (4) can be accomplished with a 2HDM model as considered in [24]. This introduces two $SU(2)_L$ doublets H_1 and H_2; the first is "SM-like," coupling to SM fermions (ψ_i), while the second has no fermion couplings, but couples to X. Schematically,

$$\mathcal{L} \supset D_\mu H_1^\dagger D^\mu H_1 + y_{ij} H_1 \psi_i \psi_j + D_X^\mu H_2^\dagger D_{X,\mu} H_2, \quad (9)$$

where the covariant derivative acting on H_2 contains a $U(1)_X$ contribution. To avoid introducing extra EWSB into the $SM + X$ EFT requires the light scalar Higgs to be aligned with the direction of EWSB. In the notation of [37], this is the "decoupling limit" $\cos(\alpha - \beta) = 0$, where α is the angle between the neutral components of H_2, H_1 and the scalar mass states, and β is the angle between H_1, H_2 and the direction of EWSB. Then, writing $H_2 = s_\beta H + c_\beta \tilde{H}$, where H is the SM Higgs doublet and $\tilde{H}$ consists of heavier states that do not obtain a VEV, we can integrate out $\tilde{H}$ to obtain an effective coupling of the form of (4),

$$(D_{X,\mu}H_2)^\dagger(D_X^\mu H_2) \supset \underbrace{-\frac{g_X}{g/2c_W}s_\beta^2}_{\varepsilon_Z} X_\mu H^\dagger i\overset{\leftrightarrow}{D}{}_X^\mu H. \quad (10)$$

The mass of X in this model receives two independent contributions: one from the VEV of H, and another from a Stueckelberg mass term in the Lagrangian. In more general 2HDM models, where h is not aligned with the direction of EWSB, we obtain couplings beyond (3) and (4), allowing enhanced Higgs decay rates at tree level [19–21].

Lastly, one might wonder if it is possible to remove the dangerous m_X^{-1}-enhanced terms by charging additional fermions under $U(1)_X$, resulting in a conserved current. The simplest way of doing it is suggested by the conservation of the hypercharge current, that can be split into bosonic and fermionic parts:

$$0 = \partial_\mu J_Y^\mu = \partial_\mu \left(H^\dagger i \overleftrightarrow{D}^\mu H + \sum_{i \in \text{SM}} Y_i \bar{\psi}_i \gamma^\mu \psi_i \right). \quad (11)$$

Thus, if the bosonic Higgs current is completed by the addition of the fermionic hypercharge current, one would remove m_X^{-1}-enhanced terms. This would correspond to the "usual" case of the kinetic mixing/hypercharge portal.

III. FERMIONIC PROCESSES

SM fermion masses result in nonconservation of the axial part of the neutral current, so the enhancement of longitudinal X emission will occur the most in processes involving heavy fermions. For example, X-emission in the top-quark production and decay, $gg(q\bar{q}) \rightarrow t\bar{t}X$ or $t \rightarrow WbX$, will occur with the rate proportional to $\varepsilon_Z^2 m_t^2 / m_X^2$ [25,26]. Consequently, should this parameter be large, both the top-quark production cross section and its decay width will be affected. Given $O(5\%–10\%)$ accuracy in measuring the inclusive rates, setting very strong bounds on ε_Z does not seem realistic. A somewhat better sensitivity could likely be achieved employing exclusive searches of light X final states.

The most important constraints originating from the X-exchange are from $\nu_e - e$ scattering and atomic parity violation (APV). Neutrino scattering and APV are insensitive to the longitudinal mode of X, and at very small m_X the constraints are m_X independent. The most powerful limits from $\nu_e - e$ scattering are from a combination of the TEXONO [38–41], LSND [42], BOREXINO [43], GEMMA [44], and CHARM II [45] experiments. The authors of Ref. [46] summarized the limits for a $B - L$ vector and we expect similar limits to apply for a mass mixed vector with the identification, $g_{B-L} \leftrightarrow e\varepsilon_Z$. Since these are not constraining in any part of our parameter space we include these here using this rough approximation.

Researchers performing atomic parity-violation and electron parity-violation scattering experiments have long considered a mass-mixed vector as a prime target for their analyses [47,48]. We directly implement their limits here as described in [49,50].

IV. HIGGS DECAYS

The simplest processes involving bosonic couplings of X are the exotic Higgs decays $h \rightarrow ZX$ and $h \rightarrow XX$, possible for $m_X < m_h - m_Z$ and $m_X < m_h/2$ respectively. As per the discussion in previous sections, if the UV completion does not introduce extra EWSB, then the $h \rightarrow ZX$ rate is not enhanced as $m_X \rightarrow 0$, at least at tree level. For the $H^\dagger i D_X^\mu H$ coupling, the $h \rightarrow XX$ rate is likewise unenhanced at tree level. However, as we calculate in this section, loop-level effects from heavy fermions restore the small-m_X enhancement.

At one loop the effective coupling is given by the diagrams shown in Fig. 1. Note that in principle one
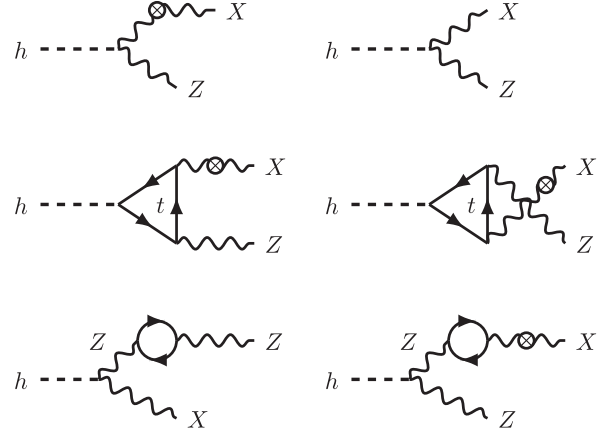
FIG. 1. Leading contributions to $h \rightarrow ZX$ decay at one-loop, where the "$\otimes$" denotes a mass mixing. At tree level there is a cancellation between the mixing term and the direct hZX coupling. Similar diagrams are present for $h \rightarrow XX$ decays.

should also include mass and field renormalization corrections on the Higgs; however these corrections all lead to corrections suppressed by extra powers of m_X and we drop them here. The effective operators are straightforward to compute with only the axial coupling contributions leading to operators of the form in (5).

After the inclusion of counterterms for the masses and the mixing parameter the divergence in the $hX_\mu Z^\mu$ is canceled, leaving behind a finite piece given by

$$C_{hZX}^{\text{loop}} = \varepsilon_Z \frac{N_c g_Z^2 m_t^2}{(4\pi)^2}, \quad (12)$$

where $g_Z \equiv e/s_W c_W$. These should be added with the tree-level couplings in (6) in either model to get the total couplings. Note that this expression has an opposite sign to the tree-level contribution and hence will interfere destructively when the two are comparable (at larger m_X).

Contrary to $hZ_\mu X^\mu$, the $hX_\mu X^\mu$ effective vertex is log-divergent and hence dependent on the UV completion. The effective vertex takes the form

$$C_{hXX}^{\text{loop}} = \varepsilon_Z^2 \frac{N_c g_Z^2 m_t^2}{(4\pi)^2} \log \frac{\Lambda^2}{m_t^2}. \quad (13)$$

These give the decay rates

$$\Gamma_{h \rightarrow ZX} = \frac{|C_{hZX}|^2 m_h}{16\pi v^2 m_X^2} \left[2w + \frac{(1-w-z)^2}{4z} \right] \sqrt{\lambda(1,w,z)}, \quad (14)$$

$$\Gamma_{h \rightarrow 2X} = \frac{|C_{hXX}|^2 m_h^3}{128\pi v^2 m_X^4} [1 - 4w + 12w^2] \sqrt{\lambda(1,w,w)}, \quad (15)$$

where $\lambda(1,w,z) \equiv 1 + w^2 + z^2 - 2zw - 2w - 2z$ and $w \equiv m_X^2/m_h^2$, $z \equiv m_Z^2/m_h^2$. Note that these are of the same form as those computed at tree level [using Eq. (6)] but

involve C_i which are not suppressed by powers of m_X. As promised, the (loop-level) decay rates are always enhanced and scale as m_X^{-2} and m_X^{-4} respectively.

Such production of X has been searched for by ATLAS [51,52]. The $h \to ZX$ only applies for a limited range of masses, $m_h - m_Z > m_X > 15$ GeV, due to the large $h \to ZZ^*$ background leading to a requirement of reconstructing the invariant mass of the decay products of X. On the other hand, $h \to XX$ applies in a broader mass range; GeV $\lesssim m_X < m_h/2$ though involves more powers of ε_Z, leading to slower improvement with luminosity. We recast the limits here in Fig. 3 with the solid lines corresponding to couplings to the $H^\dagger D_X H$ current and the dotted ones to couplings to $H^\dagger D H$.

Interestingly we find that rare Higgs decays are already a competitive constraint in the high mass range. As expected the constraints are stronger for the $H^\dagger D H$ current, already surpassing atomic parity violation. Further we note that limits for $h \to ZX$ drop at lower masses due to a cancellation between the loop- and tree-level contributions. If experimental thresholds could be lowered then such constraints would also be enhanced at smaller m_X. Lastly we note that the solid line Higgs decay constraints also apply on the 2HDM of [19] in the alignment limit, with the new loop induced constraints becoming most important at lower masses. With more data we expect future searches for rare Higgs decays will be the most constraining for heavier vectors also coupled to the more evasive $H^\dagger D_X H$ current.

V. FCNC AMPLITUDES WITH LONGITUDINAL X EMISSION

In this section we evaluate the amplitudes for FCNC decays via longitudinal X emission, using the SM $+ X$ EFT. The SM flavor changing meson decay amplitudes are suppressed by the weak scale (schematically denoted $m_{\rm EW}$), whereas on-shell X amplitudes may only be suppressed by the X coupling. This can lead to FCNC decays via an on-shell longitudinal X enhanced by $(m_{\rm EW}/m_X)^2$ relative to their SM counterparts, partially making up for the g_X^2 suppression. This effect, combined with the large statistics and high precision achieved in experimental studies of K and B decays (as opposed to e.g., Higgs boson decays), makes them a powerful tool in constraining $\{m_X, g_X\}$ parameter space.

Evaluating the down-type FCNC amplitude, $d_i d_j X$, in the SM $+ X$ EFT, involves the sum of diagrams in Fig. 2 (as a consequence of not including additional sources of EWSB there is no XW^+W^- vertex in this basis). Diagrams (a) and (b) involve the XG^+G^- and XG^+W^- couplings, while (c)–(i) come from the $X_\mu Z^\mu$ mixing. In an $R(\xi)$ gauge, the amplitude from (c)–(i) is, at leading order in external momenta, simply ε_Z times the SM Z-penguin result [53], which is finite. However, the charged Goldstone coupling in (a) results in an uncanceled logarithmic
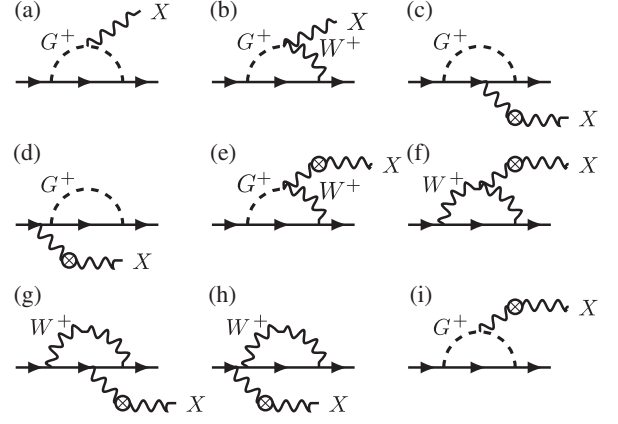
FIG. 2. (a)–(i) represents the diagrams used to compute the bsX amplitude from the SM $+ X$ EFT for X coupled to either the $H^\dagger D H$ or $H^\dagger D_X H$ current. The $\otimes$ symbol denotes a mass mixing between the X and Z. Diagrams (b) and (e) include swapping the G^+ and W^+ lines while (d) and (h) include emitting the Z from the outgoing fermion lines.

divergence. Writing the total amplitude in terms of a low-energy effective interaction, we have

$$\mathcal{L} \supset g_{d_i d_j X} \bar{d}_i \gamma_\mu P_L d_j X^\mu, \qquad (16)$$

$$g_{d_i d_j X} \simeq \frac{g^3}{2c_W} \frac{\varepsilon_Z}{16\pi^2} \sum_{q \in \{u,c,t\}} V_{q d_i} V_{q d_j}^* f(m_q^2/m_W^2), \qquad (17)$$

where f depends on the UV parameters. Assuming a wide scale separation, and the dominance of the logarithmic contribution, in the EFT one finds

$$f(x) = -\frac{x}{4} \log \frac{\Lambda^2}{m_W^2} + c_{\rm th}, \qquad (18)$$

where $c_{\rm th}$, associated with threshold corrections, is subleading to the logarithmic part in the limit where the high scale $\Lambda \gg m_W$. As usual, these threshold corrections come from both the IR scales (associated here with the weak scale) and the UV scale. Strictly speaking, it is only within a specific UV completion that one could fully identify the scale Λ and define $c_{\rm th}$. In particular, while the coefficient of the log-enhanced term in the EFT calculation is gauge independent, the other parts of the amplitude are not, illustrating that they depend on the UV completion. If additional states are at a sufficiently high scale, then we would expect the log-enhanced term to dominate, allowing concrete constraints to be set. Conversely, for smaller Λ, threshold corrections can be significant, opening the possibility of canceling it against the log-divergent piece. We discuss this more quantitatively in an explicit UV completion in Sec. VI.

In unitary gauge, only the Z-mixing diagrams contribute, and the amplitude is just given by ε_Z multiplied by the SM
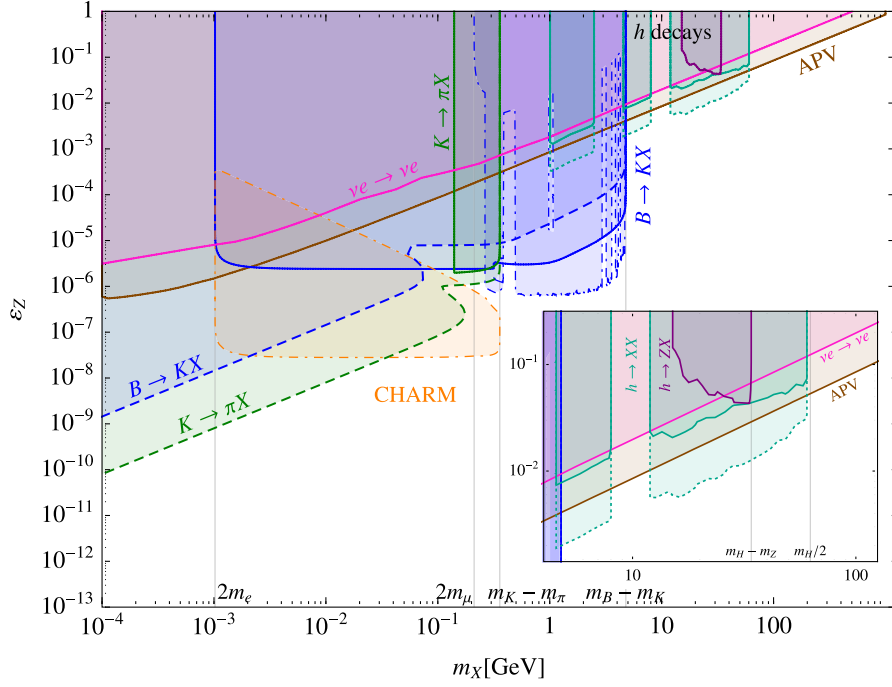
FIG. 3. Constraints on a vector X with a "mass-mixing" coupling $\varepsilon_Z m_Z^2 Z_\mu X^\mu$ to the SM Z boson. The FCNC rates from such a coupling are UV dependent—the degree to which this can affect constraints is discussed in the text. We use the limits on B decays from [55–57], from [58,59] for K decays ([60] for the SM prediction for the $K \to \pi\bar{\nu}\nu$ decay), from [61] for the CHARM beam dump, from [46] for $\nu - e$ scattering, and finally from [49,50] for computing the constraints on atomic parity violation. Solid lines denote constraints arising from visible searches, dashed from invisible searches, and dot-dashed for displaced searches. The Higgs decay constraints arise from direct searches for $h \to XX$ and $h \to ZX$ with the solid color corresponding to a vector coupled to $H^\dagger D_X H$ and the dotted to a coupling to $H^\dagger D H$ [52].

Z-penguin. This may be slightly confusing, since amplitudes for physical processes in the SM must be finite. Indeed, for the loop-induced FCNC decay of an on-shell Z-boson, $Z \to d_i \bar{d}_j$, such divergence is absent. The explanation is that the Z mass in the SM is related to its couplings, in a way that makes the divergences in the external-momenta-dependent terms in the FCNC amplitude (which we neglected above) exactly cancel the momentum-independent divergences [54]. For SM FCNC amplitudes involving off-shell Z exchange, such as $d_i \to d_j l\bar{l}$, divergences in the effective $d_i - d_j - Z$ vertex cancel against the divergences from W box diagrams [53,54]. However, m_X and g_X are independent parameters, so this cancellation will not occur for FCNC decays via an on-shell X. Consequently, computing in unitary gauge, where diagram (a) is absent, also gives rise to divergences in the SM + X EFT, resulting in the same $\log \Lambda^2/m_W^2$ contribution as the $R(\xi)$ gauge calculation.

While the top-quark loop will in general dominate, it is also useful to determine the EFT answer for the light quark contributions. If all of the up-type quarks had the same mass, then Cabibbo-Kobayashi-Maskawa unitarity would mean that the sum in Eq. (17) cancels—at least, that the EFT-calculable parts do. A UV completion with additional flavor structure could lead to the c_{th} contributions varying between

different up-type quarks. However, for a UV completion without such structure, without loss of generality we can take $f(x) \to 0$ as $x \to 0$, since all up-type quarks being massless would lead to zero total amplitude. Within the EFT, $f(x) \propto x \log x$ for small x. This means that even for an $s - d - X$ vertex, the internal up and charm contributions are always subdominant to the internal top one (unless special cancellations occur), despite the corresponding Cabibbo-Kobayashi-Maskawa elements being larger.

To summarize, FCNC amplitudes in the SM + X EFT run logarithmically, so are dependent on the UV physics. However, their generic scale is set by the X couplings in the EFT. The same structure applies for X couplings to SM fermions, as analyzed in [11]. For sufficiently light X, all of these lead to FCNC meson decays with rates enhanced by $\sim m_{\text{EW}}^2/m_X^2$ compared to competing SM processes (this is for down-type FCNCs—up-type FCNC rates are suppressed by at least additional powers of the charm mass over the weak scale). As discussed in [11], the corresponding B and K meson decays can provide strong constraints on nonrenormalizable X-SM couplings. Figure 3 illustrates these constraints for a "typical" UV model by taking $\Lambda \sim$ TeV in Eq. (18), and including only the log-enhanced term. In the next section, we will see how this relates to the results in an example UV theory. The figure also shows

other constraints arising from the SM couplings of X, including neutrino-electron scattering and parity-violation experiments, illustrating that when FCNC constraints apply, they are generically significantly stronger than other probes.

As mentioned in the Introduction, any model that results in an XW^+W^- vertex (and/or couplings to quarks) will generically contribute to FCNCs in a similar way. The ε_Z model here is illustrative in that it results in UV-divergent and m_t^2/m_W^2-enhanced amplitudes (in contrast to e.g., Wess-Zumino couplings, which lead to finite FCNC amplitudes [10,11]). As in the case of couplings to SM fermions [11], this is the generic and strongest behavior.

A. Beam-dump constraints

In our previous work [10,11], we stated that $K \to \pi X_L$ decays would be the dominant X production mechanism in proton beam-dump experiments such as CHARM [61], following the analysis in [62]. However, the details of this analysis are incorrect, since almost all of the kaons produced in such experiments will be stopped in the target before decaying.[3]

The consequences of kaon interactions in the target were investigated by the author of [63], who adopted the conservative procedure of estimating the number of kaons that decay before their first interaction. Considering X production from only these kaon decays results in a significantly smaller yield than we used in [10,11]. However, it is still the case that $K \to \pi X_L$ decays are only suppressed by $m_{\mathrm{EW}}^2/(m_X^2/g_X^2)$ compared to SM channels. On the other hand, the production rate from "π^0-like" interactions, as estimated in [61,64], is suppressed by $\sim f_\pi^2/(m_X^2/g_X^2)$ compared to the SM π^0 production rate. Consequently, even taking the small kaon survival rate from [63], X production from kaon decays still dominates over the π^0 estimate. In addition to X produced from kaon decays, there is a subdominant component arising from the production of B mesons, which decay into vectors with significantly larger boosts [65]. However, due to the smaller primary yield of B mesons (using the estimate in [63]) X production from kaons, when kinematically allowed, is typically larger. Our constraints from the CHARM beam-dump experiment (plotted in Figs. 3 and 5), which use the kaon and B efficiency estimates from [63], illustrate that beam dumps can still constrain new parameter space.

Neutrino beam experiments, in which pions and kaons are not stopped in the target, but instead focused into a collimated beam, result in a much larger kaon decay yield, and would consequently give more X production. However, the detectors in such experiments are generally set up to detect neutrino scattering events, which would constitute a

---

[3]We thank Felix Kahlhoefer for bringing this issue to our attention.

background to the X decays we want to search for. In contrast, the beam-dump mode run of CHARM [61] used a large, air-filled detector volume, yielding a basically background-free experiment (this difference is illustrated in [66]).

VI. 2HDM EXAMPLE

The $\mathrm{SM} + X$ EFT calculation in the previous section gives the "generic" scale of FCNC amplitudes. However, for UV completions in which new physics is not too far above the EW scale, it is possible that other contributions will be numerically comparable to the log-enhanced term. In particular, one might wonder about the robustness of limits for particular UV completions, as partial cancellations in the amplitude may weaken FCNC constraints. In this section, we will perform a full calculation of FCNC amplitudes (to leading order in external momenta) within a simple UV theory, illustrating these points.

As our reference model we use the 2HDM summarized in Sec. II. Calculating FCNC vertices in the full 2HDM theory, the UV divergences coming from EW penguin diagrams are canceled by diagrams involving charged Higgs exchange (Fig. 4). Computing these, we find that the total contribution to the FCNC amplitude is given by

$$g_{d_i d_j X} \simeq -\frac{g_X g^2 s_\beta^2}{16\pi^2} \sum V_{qd_i} V_{qd_j}^* f\left(\frac{m_q^2}{m_W^2}, \frac{m_{H^+}^2}{m_W^2}\right), \quad (19)$$

where

$$f(x,y) \equiv \frac{x}{4}\left\{2 + \frac{y}{y-x} - \frac{3}{x-1} + \frac{3(y-2x+1)}{(y-1)(x-1)^2}\log x \right.$$
$$\left. + \frac{y(y^2-7y+6x)}{(y-1)(y-x)^2}\log\frac{x}{y}\right\}, \quad (20)$$

and we use $x_q \equiv m_q^2/m_W^2$ and $y \equiv m_{H^+}^2/m_W^2$.
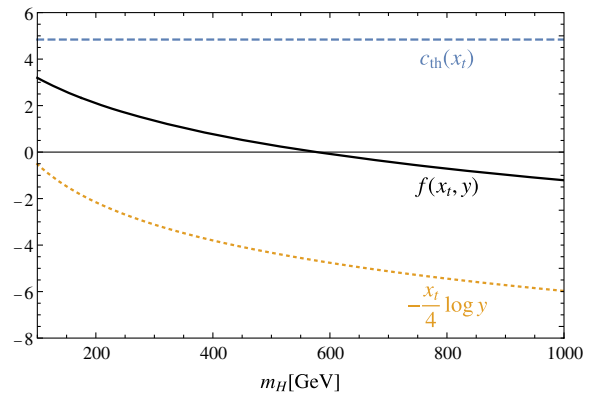
FIG. 4. Different contributions to the effective $d_i d_j X$ coupling from top loops as given in Eq. (20) (with $x_t \equiv m_t^2/m_W^2$). The dashed blue and dotted orange lines denote the threshold and large-logarithm pieces respectively while the black line denotes the full one-loop function. We see a cancellation between the threshold and running contributions around $m_H \simeq 575$ GeV beyond which the coupling is well approximated by the log-enhanced piece.

For y large, $f(x, y) \simeq -(x/4) \log y$, in agreement with the EFT result in Eq. (17). Identifying the scale Λ with m_{H^+}, we also find the threshold correction in the limit of large Λ,

$$c_{\text{th}} = \frac{x(3x^2 - 9x + 6 + (x^2 - 2x + 4) \log x)}{4(x-1)^2}. \qquad (21)$$

It is easy to see that for x given by the top mass, the sign of c_{th} is opposite to $-\frac{1}{4}x \log y$. For small enough x, we have $f \simeq x \log x$, again as expected from the EFT. Our results are in agreement with results in previous studies [24] which computed the amplitude by relating the theory to that of an axion with fermionic couplings [67]. As discussed in the previous section, the top-quark contribution is typically dominant, for both K and B decays.

The different threshold and running contributions are compared with the full expression in Fig. 4 showing a partial cancellation in the flavor changing rate at $m_{H^+} \simeq 575$ GeV for the top contribution. Note, however, that since there are additional contributions to the total FCNC decay amplitude that have a different complex phase to the top-quark contribution, the total amplitude does not pass through zero as we change m_{H^+}. For kaon decays, the next most important contribution to the sdX vertex is from the charm-quark contribution. The argument[4] of $V_{cs} V_{cd}^* \simeq -0.22 + 10^{-4}i$ is significantly smaller than that of $V_{ts} V_{td}^* \simeq 10^{-4}(-3.3 - 1.4i)$, and to a large extent this mitigates the small charm mass, $f(x_c, y)/f(x_t, y) \propto \mathcal{O}(m_c^2/m_t^2)$. Consequently, as illustrated in Fig. 5, the limits from $K^\pm \to \pi^\pm X$ decays can only be relaxed by a factor of a few by tuning m_{H^+}. On the other hand, for B decays, the charm-quark Cabibbo-Kobayashi-Maskawa product $V_{cb} V_{cs}^* \simeq 0.04 + 10^{-6}i$ has a similar magnitude to the top-quark product, $V_{tb} V_{ts}^* \simeq -0.04 + 7 \times 10^{-4}i$, and the charm loop will not play an important role (the cancellation will instead mostly be lifted by external momentum corrections, which are suppressed by $\sim m_b^2/m_W^2$ compared to the top contribution).

Figure 5 illustrates how these cancellations affect the experimental constraints on the coupling of the new vector, for a representative value of $m_X = 300$ MeV (where both K and B decay constraints apply). As noted above, for "generic" UV completions, the FCNC constraints are significantly stronger than other experimental probes. The figure shows that $B \to KX$ and $K_L \to \pi^0 X$ constraints (the latter process is CP violating, so only depends on the imaginary part of the amplitude, which generically goes through zero) can be significantly relaxed at the same value of m_{H^+}. However, the $K^\pm \to \pi^\pm X$ constraints are not significantly canceled around that point; overall, the limit

---
[4]We use the Particle Data Group parametrization of the Cabibbo-Kobayashi-Maskawa matrix [68].
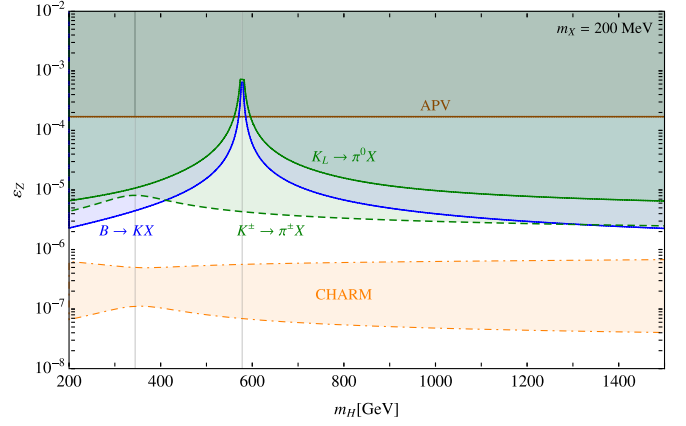
FIG. 5. Constraints on ε_Z in the 2HDM model of Sec. VI, for a light vector mass of $m_X = 300$ MeV. As discussed in the text, varying the UV physics (here, the charged Higgs mass) changes the FCNC amplitudes involving X, and consequently changes FCNC meson decay rates. For $K^+ \to \pi^+ X$ decays, the impact is mild, whereas for $B \to KX$ and $K_L \to \pi^0 X$ decays, there is a specific charged Higgs mass for which the rates are significantly reduced. We also include constraints from the CHARM beam-dump experiment [61] which are dominated by production of both K^+ and K_L. Also plotted are atomic parity-violation constraints [49,50] on ε_Z, which do not depend on the UV completion—these are always weaker than K^+ decay constraints, and can only compete with the other meson decays in a narrow m_{H^+} range.

on g_X varies only by a factor ~ 2 across the entire range of m_{H^+}. Nevertheless, the reduction of the log contributions due to threshold corrections is clearly an important effect. While constraints in Fig. 3 are plotted using the simplified form $f(x_t, y) = -(x_t/4) \times \log(\text{TeV}^2/m_W^2)$, the same value of $f(x, y)$ in the UV complete version is achieved with $m_{H^+} \simeq 7.5$ TeV.

While these calculations were performed in the context of a particular UV completion, the generic point that different components of the amplitude have different complex phases can be seen within the EFT. Consequently, if FCNCs in the UV completion are dominantly controlled by one parameter (m_{H^+} in our 2HDM example), then varying this parameter will generically not result in the amplitude passing through zero. Thus, unless the UV completion has additional flavor structure that enables it to arrange such a cancellation, and/or multiple parameters which affect the different-phase components in different ways, FCNC amplitudes can generically only be canceled by a similar degree to that derived here.

Another point illustrated by this UV completion is that the scale of new physics has to be sufficiently low for the partial cancellations to occur. For the case of extended Higgs sectors, the current constraints on the mass of the new charged Higgs states range from ~ 200–600 GeV depending on the details of the Higgs sector (see [69–71] for CMS searches and [72–74] for corresponding ATLAS searches). These limits are statistics dominated and should

improve with the high luminosity LHC run. In the considered UV completion, the most relaxed bounds on g_X are for m_{H^+} of 575 GeV, which is within reach of the LHC.

VII. KINETIC MIXING AND FCNCS

The only fully renormalizable coupling of a new light vector to the SM is via "kinetic mixing" with the hypercharge gauge boson,

$$\mathcal{L} \supset \frac{1}{2}\varepsilon_Y X_{\mu\nu}B^{\mu\nu} \qquad (22)$$

(if neutrinos are Dirac, then a coupling to the $B - L$ current is also renormalizable). Defining electromagnetic and weak neutral currents of the SM as $\mathcal{L} \supset A_\mu J_{\text{EM}}^\mu + Z_\mu J_Z^\mu$, to first order in the small mixing ε_Y, we can perform field redefinitions so that the new light spin-1 state has couplings

$$\mathcal{L} \supset \varepsilon_Y X_\mu \left(J_{\text{EM}}^\mu \cos\theta_W + \frac{m_X^2}{m_Z^2} J_Z^\mu \sin\theta_W \right), \qquad (23)$$

where θ_W is the weak mixing angle. While a coupling to the (nonconserved) neutral current leads to energy/m_X-enhanced longitudinal amplitudes, the m_X^2/m_Z^2 suppression of this coupling means that such amplitudes are suppressed by $m_X E/m_Z^2$ overall, and hence vanish for $m_X \to 0$ as required by renormalizability.

Most treatments of "dark photons"—new vectors with a coupling to the EM current in the low-energy (sub-EW-scale) SM—do not consider the small neutral current coupling that would arise from hypercharge mixing. One reason is that, in nonrenormalizable SM $+ X$ models, these couplings are not necessarily linked (e.g., one could always add a kinetic mixing to the models in the previous section). Another is that, while the neutral current coupling does give some experimentally distinct signatures, the m_X^2/m_Z^2 suppression means that, for $m_X \ll m_Z$, these are generally less important than the EM coupling signatures.

This point is illustrated by FCNC meson decays, which, as discussed in previous sections, are generally the strongest probes of a light vector's neutral current coupling. For kaon decays, the $K^+ \to \pi^+\gamma^*$ amplitude can be computed in chiral perturbation theory, using information on the $K \to 3\pi$ amplitude as input [75]. This gives the FCNC amplitude from the EM current coupling of X [6]. The amplitude from the neutral current couplings is given by the usual EW penguin contribution. Due to the m_X^2 suppression of the neutral current coupling in (23), both of these are $\propto m_X^2$. However, the penguin contribution is suppressed by $V_{ts}V_{td}^*$, which has magnitude $\sim 4 \times 10^{-4}$, whereas the γ^* amplitude is only suppressed by the Cabibbo angle. Hence, the neutral current contribution to these decays is subdominant to the dark photon contribution. The same is true

for $K_S \to \pi X$ decays. For $K_L \to \pi^0 X$ decays, which are CP violating, the neutral current term dominates; however, the experimental limits on these decays are comparable to those for $K^+ \to \pi^+ X$, so the latter will generally be a better probe of a hypercharge-mixed vector. In the end, it turns out that the kaon decays do not put any additional restrictions on dark photons compared to standard "bump hunt" searches, with the exception of models with a large $X \to invisible$ channel, where the competing SM rate, $K^+ \to \pi^+\nu\bar{\nu}$, has a very small branching.

$B \to KX$ constraints on the kinetic mixing are even less important than the kaon constraints. $B \to K\gamma$ decay occurs with the branching ratio of $\simeq 4 \times 10^{-5}$, and the corresponding decay to a dark photon will be smaller by a factor of $(\varepsilon_Y \cos\theta_W)^2$. Current experimental constraints require $\varepsilon_Y \lesssim 10^{-3}$ over the relevant mass range, which renders the B decays well outside experimental capabilities. Contributions of neutral currents do not change this conclusion.

VIII. CONCLUSIONS

We have discussed some of the simplest ways of coupling new light vectors to the bosonic sector of the SM and their phenomenological consequences. In particular, we have focused on the lowest-dimensional, SM-gauge-invariant currents to which a new vector can couple. Besides kinetic mixing, the only two nontrivial currents are $H^\dagger DH$ and $H^\dagger D_X H$. Coupling a light vector, X_μ, to these currents leads to an effective $Z - X$ mass mixing, as well as couplings of X to the scalar Higgs. The most observationally significant effects of these couplings come about through m_X^{-1}-enhanced longitudinal X emission, analogously to couplings to nonconserved fermionic currents [11].

An important property of the $H^\dagger D_{(X)} H$ currents is that they are conserved in the purely bosonic sector of the SM for single-X emissions. Hence, one should not expect an enhancement of the longitudinal X emission at tree level. Nevertheless, this property is broken by quantum corrections and m_X^{-1}-behavior is present when fermions are included, as the Yukawa/mass terms break current conservation. An important place to look for the source of the constraints is the loop-induced processes which can profit from the high energies available in the virtual states. Loops of top quarks can induce important signals for both currents of interest and we highlight their potential to probe such vectors.

For sufficiently light vectors, flavor changing decays of the K and B mesons are extremely sensitive probes of bosonic couplings, imposing more stringent constraints than parity-violation or scattering experiments. Applying the EFT calculation to the SM $+ X$ theory, we compute the FCNC amplitudes, identifying the leading $\log(\Lambda/m_W)$ behavior. To explore the relation of the effective theory to its UV completions and the possibility of a cancellation

eliminating these constraints, we study a two Higgs doublet UV completion in detail, with one of the Higgs fields charged under $U(1)_X$. We find that the threshold corrections, as it is often the case, contribute with the opposite sign to the logarithmically enhanced terms. At $m_{H^+} \sim 575$ GeV there is nearly perfect cancellation of the bsX amplitude. We argue, however, that such cancellation is not universally applicable to all enhanced $d_i d_j X$ amplitudes. Up to the caveat of an exotic case of UV completion with additional flavor structure, FCNC contributions with different complex phases cannot generically be simultaneously canceled, leading to the conclusion that $K^+ \to \pi^+ X$ amplitudes can only be suppressed by a factor of a few.

Another possibility raised in the literature [24] is that FCNCs could be canceled between nonrenormalizable and renormalizable (kinetic mixing) couplings of the same vector. However, such tuning is only relevant for $K^\pm \to \pi^\pm X$ decays (and even then can only reduce the rate by a factor ~ 10); B-physics is far less affected by the kinetic mixing operators (and moreover $B \to KX$ and $B \to K^*X$ decays are affected differently).

While we performed FCNC calculations for particular vector coupling models, these conclusions apply more generally. Quark FCNC amplitudes depend on the XW^+W^- coupling (and the quark couplings) of the new vector, so any models giving that coupling will lead to the similar decays. Other couplings of X to SM bosons have smaller effects; a XZZ vertex only contributes to less important low-energy processes, while processes involving vertices of X with three SM gauge bosons are suppressed by additional powers of the weak scale (or extra loop factors). There can also be dimension-4 couplings involving more than one X, such as an XXW^+W^- vertex. However, if the X-SM couplings are all suppressed by some small parameter g_X, then in most UV completions, XX-SM vertices will be suppressed by g_X^2, limiting their capability to constrain these couplings.

For heavier vectors, exotic Higgs decays provide a relatively clean probe, as long as the vector decays to SM states. We studied the decays for both currents, finding that only for $H^\dagger DH$ can the tree-level decays have a longitudinal enhancement, observable in $h \to XX$ decays. Nevertheless, approximate current conservation is broken at one loop leading to enhanced $h \to ZX$ and $h \to XX$ decays for both currents. These conclusions rely on our assumption that the theory does not have additional sources of electroweak symmetry breaking other than the SM Higgs. If this is violated (e.g., by a generic two Higgs doublet model), then enhanced decays can occur already at tree level. Overall, we clarify how Higgs decay rates to X can vary across different models, and we highlight their potential to probe vectors above the few-GeV meson threshold.

ACKNOWLEDGMENTS

[1] C. Boehm and P. Fayet, Nucl. Phys. **B683**, 219 (2004).
[2] M. Pospelov, A. Ritz, and M. B. Voloshin, Phys. Lett. B **662**, 53 (2008).
[3] N. Arkani-Hamed, D. P. Finkbeiner, T. R. Slatyer, and N. Weiner, Phys. Rev. D **79**, 015014 (2009).
[4] S. N. Gninenko and N. V. Krasnikov, Phys. Lett. B **513**, 119 (2001).
[5] Y. Kahn, M. Schmitt, and T. M. P. Tait, Phys. Rev. D **78**, 115002 (2008).
[6] M. Pospelov, Phys. Rev. D **80**, 095002 (2009).
[7] D. Tucker-Smith and I. Yavin, Phys. Rev. D **83**, 101702 (2011).
[8] B. Batell, D. McKeen, and M. Pospelov, Phys. Rev. Lett. **107**, 011803 (2011).
[9] J. L. Feng, B. Fornal, I. Galon, S. Gardner, J. Smolinsky, T. M. P. Tait, and P. Tanedo, Phys. Rev. D **95**, 035017 (2017).
[10] J. A. Dror, R. Lasenby, and M. Pospelov, Phys. Rev. Lett. **119**, 141803 (2017).
[11] J. A. Dror, R. Lasenby, and M. Pospelov, Phys. Rev. D **96**, 075036 (2017).
[12] A. Ismail and A. Katz, J. High Energy Phys. 04 (2018) 122.

[13] A. Ismail, A. Katz, and D. Racco, J. High Energy Phys. 10 (2017) 165.
[14] P. J. Fox, I. Low, and Y. Zhang, J. High Energy Phys. 03 (2018) 074.
[15] P. Fayet, Phys. Rev. D **74**, 054034 (2006).
[16] P. Fayet, Phys. Rev. D **75**, 115017 (2007).
[17] V. Barger, C.-W. Chiang, W.-Y. Keung, and D. Marfatia, Phys. Rev. Lett. **108**, 081802 (2012).
[18] S. G. Karshenboim, D. McKeen, and M. Pospelov, Phys. Rev. D **90**, 073004 (2014); **90**, 079905(A) (2014).
[19] H. Davoudiasl, H.-S. Lee, and W. J. Marciano, Phys. Rev. D **85**, 115019 (2012).
[20] H. Davoudiasl, H.-S. Lee, I. Lewis, and W. J. Marciano, Phys. Rev. D **88**, 015022 (2013).
[21] H. Davoudiasl, H.-S. Lee, and W. J. Marciano, Phys. Rev. D **92**, 055005 (2015).
[22] B. Holdom, Phys. Lett. **166B**, 196 (1986).
[23] H.-S. Lee and M. Sher, Phys. Rev. D **87**, 115009 (2013).
[24] H. Davoudiasl, H.-S. Lee, and W. J. Marciano, Phys. Rev. D **89**, 095006 (2014).

[25] D. Kim, H.-S. Lee, and M. Park, J. High Energy Phys. 03 (2015) 134.

[26] K. Kong, H.-S. Lee, and M. Park, Phys. Rev. D **89**, 074007 (2014).

[27] H. Davoudiasl, W. J. Marciano, R. Ramos, and M. Sher, Phys. Rev. D **89**, 115008 (2014).

[28] F. Xu, J. High Energy Phys. 06 (2015) 170.

[29] E. Izaguirre and I. Yavin, Phys. Rev. D **92**, 035014 (2015).

[30] L. Delle Rose, S. Khalil, and S. Moretti, Phys. Rev. D **96**, 115024 (2017).

[31] M. D. Campos, D. Cogollo, M. Lindner, T. Melo, F. S. Queiroz, and W. Rodejohann, J. High Energy Phys. 08 (2017) 092.

[32] M. Abdullah, J. B. Dent, B. Dutta, G. L. Kane, S. Liao, and L. E. Strigari, Phys. Rev. D **98**, 015005 (2018).

[33] E. Bertuzzo, S. Jana, P. A. N. Machado, and R. Zukanovich Funchal, Phys. Rev. Lett. **121**, 241801 (2018).

[34] P. Souder and K. D. Paschke, Front. Phys. (Beijing) **11**, 111301 (2016).

[35] M. S. Safronova, D. Budker, D. DeMille, D. F. J. Kimball, A. Derevianko, and C. W. Clark, Rev. Mod. Phys. **90**, 025008 (2018).

[36] P. J. Fox, J. Liu, D. Tucker-Smith, and N. Weiner, Phys. Rev. D **84**, 115006 (2011).

[37] G. C. Branco, P. M. Ferreira, L. Lavoura, M. N. Rebelo, M. Sher, and J. P. Silva, Phys. Rep. **516**, 1 (2012).

[38] M. Deniz et al. (TEXONO Collaboration), Phys. Rev. D **81**, 072001 (2010).

[39] H. B. Li et al. (TEXONO Collaboration), Phys. Rev. Lett. **90**, 131802 (2003).

[40] H. T. Wong et al. (TEXONO Collaboration), Phys. Rev. D **75**, 012001 (2007).

[41] J.-W. Chen, H.-C. Chi, H.-B. Li, C. P. Liu, L. Singh, H. T. Wong, C.-L. Wu, and C.-P. Wu, Phys. Rev. D **90**, 011301 (2014).

[42] L. B. Auerbach et al. (LSND Collaboration), Phys. Rev. D **63**, 112001 (2001).

[43] G. Bellini et al., Phys. Rev. Lett. **107**, 141302 (2011).

[44] A. G. Beda, E. V. Demidova, A. S. Starostin, V. B. Brudanin, V. G. Egorov, D. V. Medvedev, M. V. Shirchenko, and T. Vylov, Phys. Part. Nucl. Lett. **7**, 406 (2010).

[45] P. Vilain et al. (CHARM-II Collaboration), Phys. Lett. B **302**, 351 (1993).

[46] S. Bilmis, I. Turan, T. M. Aliev, M. Deniz, L. Singh, and H. T. Wong, Phys. Rev. D **92**, 033009 (2015).

[47] J. Benesch et al. (MOLLER Collaboration), arXiv:1411.4088.

[48] T. Aoki et al., Appl. Phys. **123**, 120 (2017).

[49] S. G. Porsev, K. Beloy, and A. Derevianko, Phys. Rev. Lett. **102**, 181601 (2009).

[50] C. Bouchiat and P. Fayet, Phys. Lett. B **608**, 87 (2005).

[51] G. Aad et al. (ATLAS Collaboration), Phys. Rev. D **92**, 092001 (2015).

[52] M. Aaboud et al. (ATLAS Collaboration), J. High Energy Phys. 06 (2018) 166.

[53] T. Inami and C. S. Lim, Prog. Theor. Phys. **65**, 297 (1981); **65**, 1772(E) (1981).

[54] X.-G. He, J. Tandean, and G. Valencia, Eur. Phys. J. C **64**, 681 (2009).

[55] J. Grygier et al. (Belle Collaboration), Phys. Rev. D **96**, 091101 (2017).

[56] B. Aubert et al. (BABAR Collaboration), Phys. Rev. Lett. **102**, 091803 (2009).

[57] R. Aaij et al. (LHCb Collaboration), Phys. Rev. D **95**, 071101 (2017).

[58] A. V. Artamonov et al. (E949 Collaboration), Phys. Rev. Lett. **101**, 191802 (2008).

[59] A. Alavi-Harati et al. (KTeV Collaboration), Phys. Rev. Lett. **93**, 021805 (2004).

[60] A. Crivellin, G. D'Ambrosio, T. Kitahara, and U. Nierste, Phys. Rev. D **96**, 015023 (2017).

[61] F. Bergsma et al. (CHARM Collaboration), Phys. Lett. B **157B**, 458 (1985).

[62] M. J. Dolan, F. Kahlhoefer, C. McCabe, and K. Schmidt-Hoberg, J. High Energy Phys. 03 (2015) 171; 07 (2015) 103(E).

[63] M. W. Winkler, Phys. Rev. D **99**, 015018 (2019).

[64] R. Essig, R. Harnik, J. Kaplan, and N. Toro, Phys. Rev. D **82**, 113008 (2010).

[65] B. Dbrich, F. Ertas, F. Kahlhoefer, and T. Spadaro, Phys. Lett. B **790**, 537 (2019).

[66] F. Bergsma et al. (CHARM Collaboration), Phys. Lett. B **128B**, 361 (1983).

[67] M. Freytsis, Z. Ligeti, and J. Thaler, Phys. Rev. D **81**, 034001 (2010).

[68] M. Tanabashi et al. (Particle Data Group), Phys. Rev. D **98**, 030001 (2018).

[69] V. Khachatryan et al. (CMS Collaboration), J. High Energy Phys. 11 (2015) 018.

[70] V. Khachatryan et al. (CMS Collaboration), J. High Energy Phys. 12 (2015) 178.

[71] A. M. Sirunyan et al. (CMS Collaboration), Phys. Rev. Lett. **119**, 141802 (2017).

[72] G. Aad et al. (ATLAS Collaboration), J. High Energy Phys. 03 (2016) 127.

[73] G. Aad et al. (ATLAS Collaboration), Phys. Rev. Lett. **114**, 231801 (2015).

[74] M. Aaboud et al. (ATLAS Collaboration), Phys. Lett. B **759**, 555 (2016).

[75] G. D'Ambrosio, G. Ecker, G. Isidori, and J. Portoles, J. High Energy Phys. 08 (1998) 004.